International Journal of Computing and Digital Systems
ISSN (2210-142X)
Int. J. Com. Dig. Sys. 12, No.1 (Aug-2022)

https://dx.doi.org/10.12785/ijcds/120152

Computer Aided Diagnosis of Melanoma Based on the ABCD Rule

Majd Tahat[1], Belal Abuata[2] and Maryam Nuser[1]

[1]*Department of Information Systems, Yarmouk University, Irbid, JORDAN*

[2]*Department of Information Technology, Yarmouk University, Irbid, JORDAN*

Received 18 Nov. 2021, Revised 9 May 2022, Accepted 15 Jul. 2022, Published 6 Aug. 2022

Abstract: Malignant melanoma is a very serious dermatological disease, which is rare but away more deadly skin cancer. Melanoma is the most dangerous form of skin cancer, while curable with early stages detection. Beside professional specialists that are capable of precisely identifying the disease, automated systems are also capable of recognizing disease which might save lives and reduce costs. Toward this goal, in this research, a classifier model based on support vector machine (SVM) with radial basis function kernel was fed with image features and class labels to predict the presence or absence of the malignancy in dermoscopy images. Based on this classifier, ABCD features (Asymmetry, Border, Color and Diameter) and texture features derived from the Haralick texture features calculated from Gray Level Co-occurrence Matrix were investigated to find the best features that could increase the accuracy of the diagnosis process. Eventually, results concluded 12 texture features with highest efficiency. In addition, results show that the new added texture features did improve the accuracy by a `9.6%` than the common ABCD rule from `84%` to `93.6%`.

Keywords: Melanoma Diagnosis, Texture Features, Support Vector Machine, ABCD Features

1. Introduction

Malignant melanoma (MM) is the most dangerous type of SKIN cancers, responsible for approximately four-fifths of the deaths. In its advanced stages, melanoma is untreatable, and the treatment includes being solely palliative, immunotherapy, surgery, and chemotherapy [1]. However, non-melanoma skin cancers, especially squamous or basal cell cancers are highly curable. Despite melanoma‘s rapid spread to other parts of the body, it would also be highly curable if recognized early and treated decently [2]. One out of each five Americans will likely get skin cancer in their lifetime as stated by skin cancer foundation. Worthy of attention, white people are commonly harmed by MM due to heavy direct sun exposure [3].

The dermoscopy images are used to recognize melanoma and other pigmented skin lesions (PSLs) [4], [5]. In clinical processes, dermatologists utilize such images to clearly visualize the lesions. Despite the fact that this device displays clear features of skin lesions, yet it is very difficult to differentiate between various melanoma types, even most professional dermatologists have accuracy under 85% [4]. Therefore, many melanoma cases are not diagnosed fairly. To clinically diagnose lesions, experienced dermatologists depend on pattern recognition, history, and laboratory parameters. To automatically diagnose lesions, computer-aided diagnostic (CAD) systems depend on different classification techniques such as: Artificial Neural Network (ANN), Support Vector Machine (SVM) and feature selection, deep learning or hybrid approaches [6], [7], [8], [9], but the main steps in any melanoma recognition system are: preprocessing, lesion segmentation, feature extraction, feature selection, and finally classification.

The main objective of the research aims to study texture features that should be merged with the ABCD features for the purpose of enhancing the overall malignant melanoma diagnosis process

2. Background

Recently, health data analysis is an issue that researches focus on due to several complexities that faces analysts and big data miners [10], [11], [12]. Classification problems is one of the targeted areas [13] that helps physicians in decision making. This research focuses on lesion classification. Image processing and analysis is vital for lesion classification in any automated system. Lesion classification outcome can be binary (benign/malignant or non-suspicious/suspicious for malignancy), ternary (common nevus/dysplastic nevus/melanoma) or n-array, which defines different skin diseases. Consequently, these outcomes represent types of pigmented skin lesions (PSLs) that a system

E-mail address: tahat.majd@gmail.com, belalabuata@yu.edu.jo, mnuser@yu.edu.jo

is trained to differentiate.

Maglogiannis and Doukas at [14] introduced classification outputs of various CAD systems and present a unified comparison of eleven classifiers on a group of feature descriptors (using several feature selection approaches) utilizing a database of 3639 dermoscopic images. The eleven selected classifiers were the most common classifier sets utilized in the PSL computerized analysis, consisting of decision trees, SVM, regression analysis and neural networks among others. The comparison was performed in three sub-experiments, which compute the number of resulted classes. The first two experiments were common nevus classes/common nevus and dysplastic/melanoma, while the third experiment integrated all three classes. Consequently, SVM demonstrated the best general performance.

Numerous other studies from the CAD systems and classification groups have compared two/three or more classifiers. Consequently, the comparisons among SVM and artificial neural networks (ANN) have been conducted in many papers [15], [16]. In general, the classifiers performance was slightly varied. Whereas discriminant analysis (DA) was compared in several studies with ANN in [17] and to both SVM and ANN in [18], showing even or slightly worse performance. Bayesian classifier was assessed against SVM in [19] and against ANN and k-nearest neighbor (KNN) in [20]. It was shown to fall behind the ANN but exceeded the KNN method performance. Kassem et al. [21] compared traditional machine learning methods and deep learning methods for skin lesion classification. They explored the main challenges of evaluating skin lesion segmentation and classification methods such as small datasets, ad hoc image selection and racial bias.

Many other studies from the CAD systems and Classification categories have made improvements on the medical diagnosis and treatment field. In particular, the performance of the artificial neural networks (ANN) has been improved in [22]. These improvements have been done by applying deep learning algorithms at PSLs by extracting the texture and color features from skin lesions images. Results showed that their system was robust compared to other CBIR systems and it can be used to help clinical experts. Another decision support system that used deep feature learning on dermoscopic images was presented by Kharazmi et al. in [23]. They proposed a new framework for comprehensive detection of cutaneous vessels. The classification was binary such that the system either identified an absence or presence of vasculature. The framework demonstrated superior performance of 95.4% detection accuracy.

For classifying PSL as malignant or benign, a new method was proposed which is based on the ABCD rule [24]. Two classifiers were utilized in the experiments: the KNN combined with a Decision Tree classifier (KNN-DT) and the KNN classifier alone [25]. The approach was applied on two publicly available datasets of PSL images.

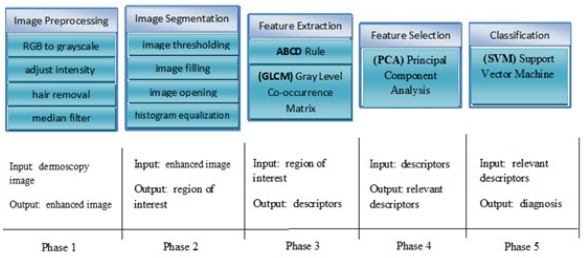

Figure 1. The research phases that are followed in this research

In summary, authors declared that the initial experimental results were promising, and claimed that the approach can reach a classification accuracy of up to 96.71% [26]. Another improvement to the ABCD rule was described in [27]. The main addition of the new algorithm is the deep use of Persistent Homology process, which ensures an extensive analysis of the skin lesion. The algorithm has been tested on a 107 melanocytic lesions dataset, with fine results; authors conclude that this method needs more tests and investigation.

In conclusion, one of the weaknesses and gaps of the preceding researches is that there is a need for more symptoms and parameters to enhance the diagnoses process. To fulfil this gap, this research was presented which aims to improve malignant melanoma diagnosis process through studying texture features that should be merged with the ABCD features, using SVM classifier to predict images class labels.

3. Research Methodology

We have employed five phases of operation in order to achieve an accurate retrieval of images of skin tumors, which include preprocessing, segmentation, features extraction, features selection and classification. Fig. 1 shows the research main steps.

A. *Data Sample*

The digital dermoscopy images and their case histories symptoms and treatment plans were gathered from two sources: the international skin imaging collaboration project (https://api.isic-archive.com/api/docs/swagger/) and from the international atlas of dermoscopy and dermatoscopy website (https://www.dermoscopyatlas.com/), which is an educational activity of the skin cancer college of Australia and New Zealand. Lastly, 220 images were investigated which were fairly divided over malignant melanoma and common nevus with 110 images for each, and they were resized to 512×512 pixels. The previously mentioned research phases were applied to the collected data as in the following section.

4. Experiments

A. *Preprocessing*

The first phase that was applied to the raw imaging data is preprocessing which aims to enhance the image and it consisted of the following steps:

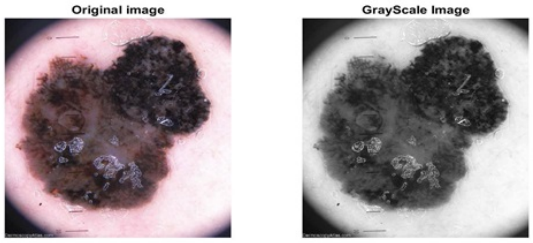

Figure 2. Converting RGB image to grayscale image

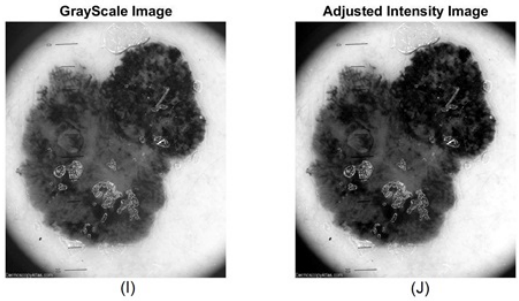

Figure 3. Adjusting grayscale image intensity

1) Grayscale image

It is an array whose values represent intensities within some range. However, the main goal of converting color map images to gray level is to distinguish visual features that can't be defined in true colored images. Fig. 2 shows the result of converting an RGB image from the data sample to gray level image.

2) Intensity Adjustment

As demonstrated in Fig. 3, at this step, the intensity values in grayscale image (Fig. 3.I) were adjusted to new values (Fig. 3.J), by saturating 1% of the top and the bottom of all pixel values. In other words, the contrast of the output image (Fig. 3.J) was increased.

3) Hair Removal

By observing Fig. 4, it can be noticed that beside hair, irrelevant small objects such as millimeter marks that were used to measure the diameter were removed. Hair removal process was accomplished by applying dull razor filter.

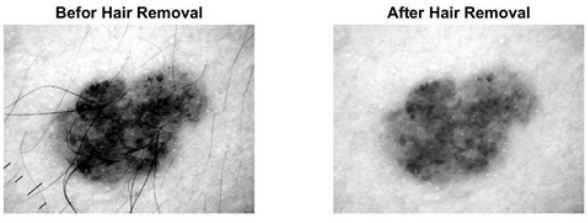

Figure 4. Applying hair removal

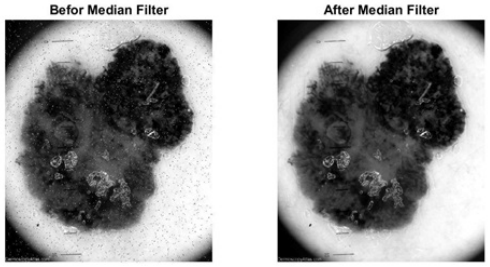

Figure 5. Applying median filter to an image

Figure 6. Image Segmentation example

4) Median Filter

As Fig. 5 indicates, median filtering is usually used in image processing to discard noise. It is a nonlinear method that mainly aims to preserve edges and reduce noise. Each output pixel carries the median value in a 3-by-3 neighborhood near the correlated pixel in the input image [28].

B. Segmentation

As represented in Fig. 6, lesions segmentation points out to the image separation into distinct regions (lesion/healthy skin) by joining pixels with related attributes. The Segmentation process helps humans in recognizing lesions boundaries. The success of image analysis depends on segmentation reliability, even though an accurate partitioning of an image is very difficult most of the time.

1) Thresholding

In this phase, the level or the global threshold that can be used to transform an intensity image into a binary image was computed as in Fig. 7 by performing Otsu's method [29] which uses the threshold to reduce the intra-class variance (within a certain segment) of the white and black pixels.

2) Image Filling

Initially, to fill image regions and holes, the binary image will be inverted since white pixels will be used to fill these holes as shown in Fig. 8. Thereafter, an algorithm that uses a morphological reconstruction will be implemented to fill image regions and holes. The algorithm, by default, uses 4-connected neighborhoods for the 2-D inverted binary image in order to assign new value to a specific pixel.

3) Image Opening

The opening is considered in image processing and computer vision as a basic structure of disposing of morphological noise [30]. Accordingly, opening disposes small

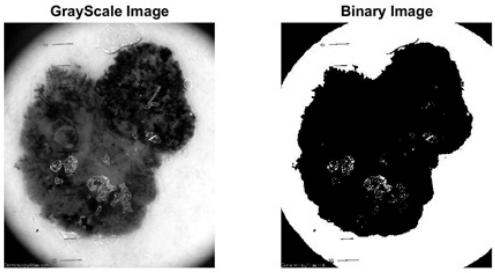

Figure 7. Image Thresholding

Figure 8. image Filling

objects from the foreground (most often taken as the bright pixels) of an image, moving them to the background. Fig. 9 is an example of image opening.

4) Histogram Equalization

Before applying histogram equalization, we determined the largest object (lesion) in the image and the boundary of it, and then we cropped it in a way that would be more beneficial for features extraction phase. Afterwards, we improved contrast using histogram equalization [31] which improves the accuracy of the (GLCM) method.

C. Features Extraction

The key to gain an effective retrieval system is to select the right features that describe each image class as uniquely as possible. The features have to be sufficient and discriminative for the description of different diseases. In our work we attempt to reflect the pigmented lesions parameters using the ABCD rule for melanoma detection combined with the common texture feature algorithm (GLCM) and other features such as (skewness, standard deviation, mean, entropy, and kurtosis).

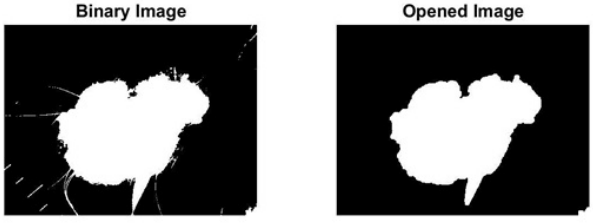

Figure 9. image Opening

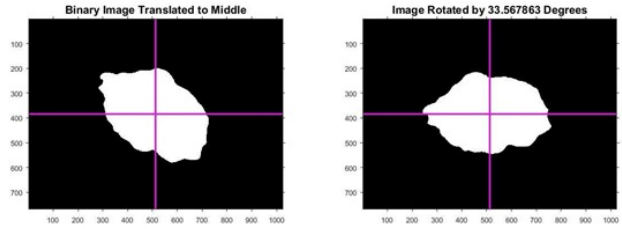

Figure 10. Lesion Rotation

1) ABCD rule of dermoscopy

Four arguments were established to be important factors for melanoma diagnoses. It is a scientific criterion that provides points for the method which contain Asymmetry-(A), Border-(B), Colors-(C) and Diameter-(D) identified in a PSL. Each identified criterion is multiplied by a weight parameter to create a Total Dermoscopic Score TDS as stated in Equation 1.

$$TDS = 1.3 \times A + 0.1 \times B + 0.5 \times C + 0.5 \times D \quad (1)$$

A TDS value above 5.45 indicates the lesion is considered probable melanoma. For an intermediate TDS score of 4.75 - 5.45 it is declared as possible melanoma and indicates benign for lesser than 4.75 [25].

a) Asymmetry

In our research we attached a new image manipulation process to measure the asymmetry precisely. Based on checking lesion properties we used the orientation of the lesion to find the angle between the major axis of the lesion and the x-axis. Eventually, we utilized this angle to identify the rotation degree that needed to match the correct parts that should be compared to check the asymmetry which is evident in Fig. 10.

Thereafter, lesion has been cut by two axes that are located so as to produce the minimal asymmetry possible in respect of borders, dermoscopic structures, and colors. The asymmetry is tested with regarding to a point below one or more axes [14].

As can be seen in Fig. 11, in (A), there is a clear absence of any asymmetry in both axes where (A,B,C,D) = (0,0,2,3) respectively which means that the ABCD score =2.5. and therefore, it is considered as normal nevus. However, in (B), Asymmetry of pigmented lesion exists in one axis; the (A,B,C,D)=(1,4,4,4) respectively, as a result the ABCD score = 5.7, and therefore it is considered as Malignant Melanoma(MM)). On the other hand, in (C), Asymmetry of lesion exists in both axes under angle of 90 degrees; the (A,B,C,D)=(2,8,5,4), the ABCD score = 7.9 and therefore, it is considered as Malignant Melanoma.

b) Borders Irregularity

The lesion is separated into eight pie-piece sections. Then, it is tested if there is an abrupt cut off of pigment

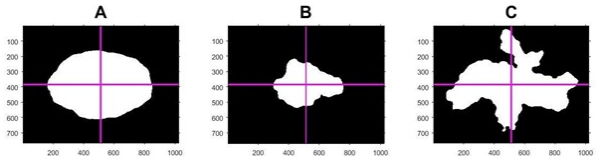

Figure 11. Evaluation of asymmetry in pigmented lesions

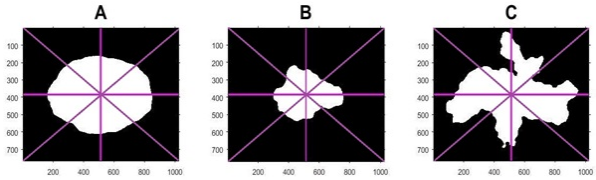

Figure 12. Evaluation of border in pigmented lesions

Figure 13. Changing background color to green

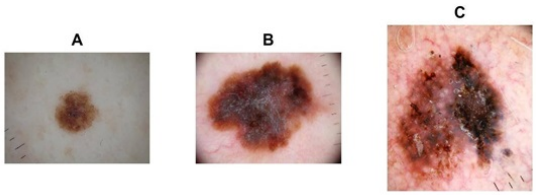

Figure 14. Evaluation of different colors in pigmented lesions

pattern at the lesion boundary or a gradual cut off. Border-based characteristics that classify the shape of the lesion are then calculated. The most common border characteristics are the border irregularity, the area, the greatest diameter, the thinness ratio [32], the variance of the distance of the border lesion points from the centroid location [33], the circularity index (CIRC) [33] and the symmetry distance (SD) [34].

As shown in Fig. 12, in (A) sharp cutoff of pigment pattern in one of eight sections/ segments (border score = 0, normal nevus) where (A,B,C,D) = (0,0,2,3) respectively which means that the ABCD score = 2.5. However, in (B) sharp cutoff of pigment pattern in four of eight sections (border score = 4, MM) thus (A,B,C,D)=(1,4,4,4) respectively as a result the ABCD score = 5.7. On the other hand, in (C) sharp cutoff of pigment pattern in all eight sections (border score =8, MM) the (A,B,C,D)=(2,8,5,4), the ABCD score = 7.9.

c) Color

Color attributes of lesion are tested, and the number of colors present is specified. Only six colors will be checked which are slate blue, dark brown, light brown, red, black and white (if it is whiter than the surrounding skin). As well as, color texture could be used for describing the nature of pigmented skin lesions.

Previous researches have examined the lesion color in different approaches, but most of them didn't discard the black color of the binary mask that surrounds the lesion, which is irrelevant for lesion color that we are testing, leading to count black in every image even though it's not presented in the lesion. This research did add a new contribution by completely removing irrelevant black color, by changing the background color from black into green which wouldn't be counted while looking for previous 6 colors (Fig. 13). Therefore, the accuracy of color and texture feature extraction processes has been increased.

As can be seen in Fig. 14, in (A) two colors (dark brown and light brown) (color score = 2, compound nevus), where (A,B,C,D) = (0,0,2,3) respectively , which means that the ABCD score = 2.5. However, in (B) four colors dark brown and light brown, black, blue-gray) (color score = 4, MM) thus (A,B,C,D)=(1,5,4,4) as a result the ABCD score = 5.8. On the other hand, in (C) Six colors (black, dark brown and light brown, red, blue-gray, white) (color score = 6, MM) hence (A,B,C,D)=(2,5,6,2), the ABCD score =7.1.

d) Diameter

If the width is greater than 6 mm then it's a sign for a probable melanoma, so any growth of a mole should be of concern. Since the dermatoscope provides the ability of tracking the marks on the image through acquisition shown in, we will use these scales to measure the diameter of the lesion [35].

In contrast, most of previous work did not measure the correct real word diameter size, since they didn't scale or convert from pixel to millimeter (mm) in particular image and that can happen only with the dermatoscope diameter marks.

To do so, we performed the following steps: first we found the longest line that passes from the lesion centroid and consider it as lesion diameter. Next the diameter length was measured, which was in pixel. Finally, as illustrated in Fig. 15 we scaled and converted an already known distance in (mm) to distance in pixel, in order to find how many pixel are in (mm) for a specific image.

2) Gray Level Co-occurrence Matrix (GLCM)

Texture analysis works as a method for classification and image analysis. It is a way of representing the spatial distribution of intensities, which makes it very beneficial in classification of similar objects (regions) in different images. Haralick texture features schieda2015diagnosis calculated from a GLCM is a popular technique to describe image texture. In this study we utilized Haralick texture features to calculate 20 texture features which are: cluster Prominence,

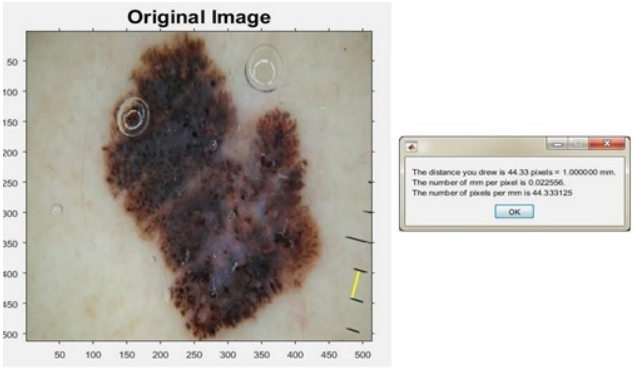

Figure 15. The scales used to calculate the actual diameter

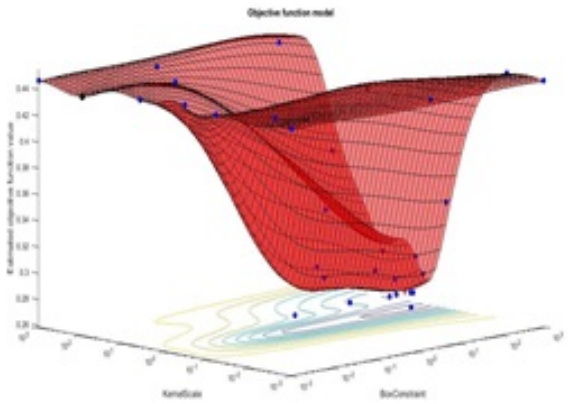

Figure 16. Hyperparameter optimization (kernelScale=gamma/ box-Constraint=cost)

contrast, entropy, correlation, homogeneity, autocorrelation, cluster shade, sum variance, difference entropy, information measure of correlation 1, information measure of correlation 2, inverse difference, and inverse difference moment, Difference variance, Dissimilarity, energy, maximum probability, sum average, sum of squares, sum entropy.

D. Features Selection

The goal of feature selection is to select a subcategory of features from the previous features selection phase which can efficiently describe the image data while minimizing bad effects from irrelevant features or noise and still provide decent prediction results. In this study, Principal component analysis (PCA) was used. PCA is a popular linear feature extractor that helps in interpreting data. It simplifies the complexity in high-dimensional data while retaining trends and patterns. Using PCA, the data will be transformed resulting in dimension reduction and this could result in better regression models. Using PCA the correlation matrix was applied as an alternative of covariance matrix. After applying this operation and measuring of variances and eigenvalues, group of main components was gathered and sorted depending on their ability to differentiate between malignant and benign lesion [36].

The features and their prediction efficiency were sorted, to prioritize them based on their prediction results. Lastly, the best 15 features with highest efficiency were chosen as follows: contrast, kurtosis, entropy, circulation, correlation, homogeneity, TDS, autocorrelation, cluster shade, sum variance, difference entropy, information measure of correlation 1, information measure of correlation 2, inverse difference, and inverse difference moment.

E. Classification

Lesion classification is the last stage in the computerized analysis ideal workflow. Lesion classification outcome can be binary, ternary or n-array, which defines different skin diseases. Consequently, these outcomes represent types (classes) of PSLs that a system is trained to differentiate. SVM radial based function (RBF) kernel classifier will be adopted in this research.

1) Support Vector Machine (SVM)

At first, we started by preparing the dataset which consists of 220 class labels with its corresponding 15 features (selected from the features selection phase). Secondly, in the training stage we have selected 114 observations from the previous step and randomly divided them into 85 observations as training set and 29 observations as testing set.

Afterwards, we optimized SVM classifier fit using k-fold Cross Validation (CV) with Bayesian optimization, so we prepared validation set using CV by randomly partitioning training set into K equal partitions, each partition was retained as the validation set for testing the model and the leftover K-1 partitions are used as training set, this step was repeated K times or (k folds) with each partition used precisely once as the validation set. Lastly, we optimized the fit to find a good fit (one with a low cross-validation loss), As a result, CV did help in optimizing the hyperplane parameters (Gamma and Cost) which prevents over fitting [37]. Gamma parameter determine how far the effect of a single training observation reaches, On the other hand, C or the cost parameter trades off misclassification of training observations versus simplicity of the decision boundary. Fig. 16 represents the hyperparameter optimization.

Finally, since data that are handled here is nonlinear, kernel SVM with radial basis function was used to build the classification model. This kernel, nonlinearly maps values into a higher dimensional space so it can deal with the situation when the relation between attributes and class labels is nonlinear.

F. Experiment Cases

To evaluate the effectiveness of the classification model used in this research, experiments on two different levels were conducted. Firstly, a comparison is done with one of the state of the art studies [36]. Case 1: The classification model has been fed with 76 data samples and 11 features

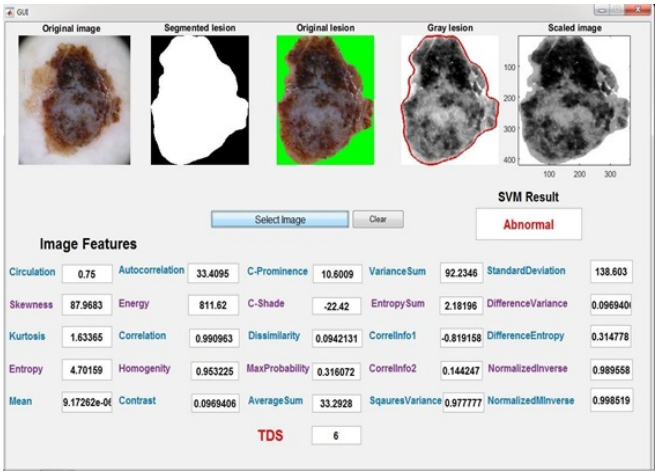

Figure 17. Graphical User Interface

(contrast, skewness, kurtosis, entropy, mean, standard deviation, circulation, energy, correlation, homogeneity, TDS). These eleven features are the same features that were used in [36]. Case 2: The same features were used, yet the number of data samples was increased from 76 to 114.

The second level of experiments aims to extract the features that will increase the accuracy of the CAD system. In case3 the classification model has been fed with 114 data samples and the common TDS feature (that hold the ABCD rule features). Case3 was compared with the same 114 data samples, and the 15 features that were chosen by the PCA method to produce Case4. In order to evaluate the diagnoses role, every one of the 220 images were separately selected and diagnosed for 4 times, each time with one of the cases that were mentioned previously. This was done with the help of the program implemented with the interface shown in Fig. 17, which consists of original image, segmented lesion, original lesion, gray lesion, scaled image, the 26 features values and SVM disease prediction result.

5. RESULTS

Table I shows the confusion matrix for the four cases. The model correctly predicted normal lesion for 79 observations and misclassified the rest of 31 normal observations as abnormal. On the other hand, the model correctly predicted abnormal lesion for 86 observations and misclassified the rest of 24 abnormal observations as normal.

TABLE I. The confusion matrix for the four cases of experiments

Experiment Case	TP	TN	FP	FN
Case 1	79	86	24	31
Case 2	101	94	16	9
Case 3	95	90	20	15
Case 4	106	100	10	4

In Case2 experiment where 114 data samples and 11 features are used; the model correctly predicted normal lesion for 101 observations and misclassified the rest of 9 normal observations as abnormal. On the other hand, the model correctly predicted abnormal lesion for 94 observations and misclassified the rest of 16 abnormal observations as normal.

For Case3 experiment (114 data samples and TDS feature). Outcomes demonstrate, the model correctly predicted normal lesion for 95 observations and misclassified the rest of 15 normal observations as abnormal. On the other hand, the model correctly predicted abnormal lesion for 90 observations and misclassified the rest of 20 abnormal observations as normal.

For the Case4 experiment (114 data samples and 15 features). Outcomes demonstrate, the model correctly predicted normal lesion for 106 observations and misclassified the rest of 4 normal observations as abnormal. On the other hand, the model correctly predicted abnormal lesion for 100 observations and misclassified the rest of 10 abnormal observations as normal.

Accuracy, recall, and precision performance measures were calculated to evaluate efficiency of the study. Accuracy value represents in general, how often is the classifier model correct. Recall value defines that, when the class label of the lesion is actually abnormal, how often the model does predict abnormal. Precision value defines that, once the model predicts abnormal image, how often is it correct. Table II shows these results for the four experiments.

TABLE II. Accuracy, recall, and precision performance measures

Experiment Case	Accuracy	Recall	Precision
Case 1	75%	76.7%	71.8%
Case 2	88.6%	86.3%	91.8%
Case 3	84%	82.6%	86.3%
Case 4	93.6%	91.3%	96.3%

F1-score value is a weighted average of the probability of detection (recall) and precision. Moreover, sometimes it's acting as an accuracy statistical measure (Table III).

TABLE III. F1-Score Results

Experiment Case	F1-Score
Case 1	74.1%
Case 2	88.9%
Case 3	84.4%
Case 4	93.8%

Initially, the research effectively succeeded in extracting the ABCD features. Resulting from applying a new manner in extracting the color feature based on discarding the black irrelevant color from the lesion background. Also the

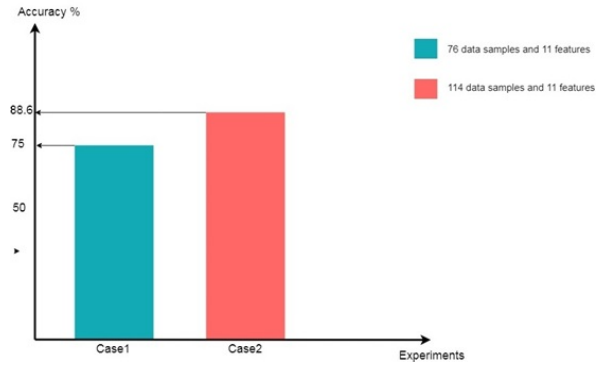

Figure 18. (Case1/ Case2) accuracy diagram

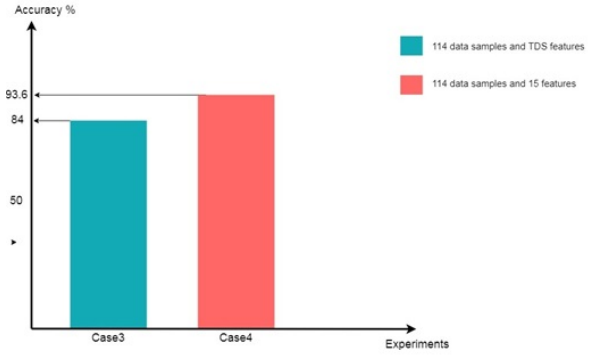

Figure 19. (Case3/ Case4) accuracy diagram

research precisely identified the lesion diameter by scaling it to a real world distance.

Secondly, GLCM features and their prediction efficiency were stored, and prioritized by PCA. Features with highest efficiency were chosen as follows: contrast, circulation, correlation, homogeneity, Autocorrelation, cluster shade, sum variance, difference entropy, information measure of correlation 1, information measure of correlation 2, inverse difference, and inverse difference moment.

Fig. 18 shows the accuracy diagram for Case1 and Case2 experiments, Case1 with an accuracy of 75% and Case2 with 88.6%. Clearly, the increasing accuracy value for Case2 refers to the number of data samples that have been fed in the classification model, since it was increased from 76 to 114 data samples (to be handled as train set and test set). As a result, this variance of values proved that the more data samples added to the classifier the more accuracy diagnose will be.

An additional result could be discussed from Case1 experiment, since the same number of features and data samples were used as in [36]. The accuracy result in their research was 92.1%, this decrease of accuracy is caused by the cross validation technique that was performed in this research which is (k-fold Cross Validation (CV) with Bayesian optimization). Instead, in their research they used the common k-fold Cross Validation. In conclusion, Bayesian optimization algorithm evidenced that it works better with big sets than small sets of data samples since it did perform very well in Case3 and Case4. Fig. 19 shows the accuracy diagram for Case3 and Case4 experiments, Case3 with an accuracy of 84% and Case4 with 93.6%. Obviously, the increasing accuracy value for Case4 refers to the number of features that have been fed to the classification model, since the most relevant 15 texture features were extracted and added with the ABCD features to the classifier.

Nevertheless, this variance of values does not prove that as the number of features increases the diagnose accuracy should also increase; because it is more likely leads to overfitting which will give false classifications [38]. Finally, the accuracy was increased as a result of the proper selection of relevant features that improves the diagnoses process and rejecting features that cause overfitting and misclassification.

In this research there is a high cost/risk associated with false negative since it deals with medical cases with serious diseases, and the best model metric to select the model specification is the recall metric. Recall is more important than precision when it's better to have less false negatives in trade off to have more false positives. Meaning, getting a false negative is very costly, and a false positive is not as much.

6. DISCUSSION

In this study, ABCD features and different texture features were investigated based on SVM with RBF kernel classifier to find the best features that could increase the accuracy of the diagnosis process. In conclusion, results show the following findings: The new added texture features did improve the accuracy by a 9.6% than the common ABCD rule from 84% to 93.6%. The texture features with highest efficiency were: contrast, circulation, correlation, homogeneity, Autocorrelation, cluster shade, sum variance, difference entropy, and information measure of correlation 1, information measure of correlation 2, inverse difference, and inverse difference moment. In addition, the proposed algorithm shows a better accuracy than some literature algorithms. [39].

The more data samples added to the classifier, the more diagnoses accuracy results will be. Bayesian optimization algorithm evidenced that it works better with big sets than small sets of data samples. Adding more features is not necessarily useful for the classification result. When the number of features increases, the more training data are needed for the classifier in order to improve the diagnoses process and prevent overfitting.

According to the results of this study, the field needs further serious attempts in building an efficient classifier with a decent cross validation method. It might also be suggested,

to study techniques like Data augmentation which increases the size of melanoma training data in a meaningful way to reduce overfitting on models. Moreover, there is a need to study the evolution and/or appearance of new lesions, which can be useful in early diagnoses of MM. Future research includes using deep learning techniques to classify such images, in addition to use another classification method such as ANN or DT besides SVM to compare the accuracy results and find the optimum artificial intelligence method in diagnosing with better accuracy.

References

[1] T. Tarver, "Cancer facts & figures 2012. american cancer society (acs)," *Journal of Consumer Health on the Internet*, vol. 16, no. 3, pp. 366–367, 2012. [Online]. Available: https://doi.org/10.1080/15398285.2012.701177

[2] M. N. E. Arani and H. Ghasemian, "A hierarchical content-based image retrieval approach to assisting decision support in clinical dermatology," *Iranian journal of electrical and computer engineering*, vol. 9, pp. 23–33, 2010.

[3] S. Pathan, K. G. Prabhu, and P. Siddalingaswamy, "Techniques and algorithms for computer aided diagnosis of pigmented skin lesions—a review," *Biomedical Signal Processing and Control*, vol. 39, pp. 237–262, 2018. [Online]. Available: https://www.sciencedirect.com/science/article/pii/S1746809417301428

[4] G. Argenziano, H. P. Soyer, S. Chimenti, R. Talamini, R. Corona, F. Sera, M. Binder, L. Cerroni, G. De Rosa, G. Ferrara *et al.*, "Dermoscopy of pigmented skin lesions: results of a consensus meeting via the internet," *Journal of the American Academy of Dermatology*, vol. 48, no. 5, pp. 679–693, 2003.

[5] F. Del Rosario, J. M. Farahi, J. Drendel, T. Buntinx-Krieg, J. Caravaglio, R. Domozych, S. Chapman, T. Braunberger, R. P. Dellavalle, D. A. Norris *et al.*, "Performance of a computer-aided digital dermoscopic image analyzer for melanoma detection in 1,076 pigmented skin lesion biopsies," *Journal of the American Academy of Dermatology*, vol. 78, no. 5, pp. 927–934, 2018.

[6] F. Warsi, R. Khanam, S. Kamya, and C. P. Suárez-Araujo, "An efficient 3d color-texture feature and neural network technique for melanoma detection," *Informatics in Medicine Unlocked*, vol. 17, p. 100176, 2019.

[7] M. A. Kadampur and S. Al Riyaee, "Skin cancer detection: Applying a deep learning based model driven architecture in the cloud for classifying dermal cell images," *Informatics in Medicine Unlocked*, vol. 18, p. 100282, 2020.

[8] A. K. Verma, S. Pal, and S. Kumar, "Comparison of skin disease prediction by feature selection using ensemble data mining techniques," *Informatics in Medicine Unlocked*, vol. 16, p. 100202, 2019.

[9] K. M. Nahar, R. M. Al-Khatib, M. A. Al-Shannaq, and M. M. Barhoush, "An efficient holy Quran recitation recognizer based on SVM learning model," *Jordanian Journal of Computers and Information Technology (JJCIT)*, vol. 6, no. 04, 2020.

[10] J. Hacker, N. Wickramasinghe, and C. Durst, "Can health 2.0 address critical healthcare challenges? insights from the case of how online social networks can assist in combatting the obesity epidemic," *Australasian journal of information systems*, vol. 21, pp. 1–17, 2017.

[11] S. A. Diwani and Z. O. Yonah, "A novel holistic disease prediction tool using best fit data mining techniques," *International Journal of Computing and Digital Systems*, vol. 6, no. 02, pp. 63–72, 2017.

[12] J. J. Shanthamalar and R. G. Ramani, "A novel approach for glaucoma disease identification through optic nerve head feature extraction and random tree classification," *International Journal of Computing and Digital Systems*, vol. 10, 2021.

[13] M. Nuser and E. Al-Horani, "Medical documents classification using topic modeling," *Indonesian Journal of Electrical Engineering and Computer Science*, vol. 17, p. 1524, 2020.

[14] I. Maglogiannis and C. N. Doukas, "Overview of advanced computer vision systems for skin lesions characterization," *IEEE transactions on information technology in biomedicine*, vol. 13, no. 5, pp. 721–733, 2009.

[15] B. J. Janney, S. E. Roslin, and M. J. Shelcy, "A comparative analysis of skin cancer detection based on svm, ann and naive bayes classifier," in *2018 International Conference on Recent Innovations in Electrical, Electronics & Communication Engineering (ICRIEECE)*. IEEE, 2018, pp. 1694–1699.

[16] Q. T. Pham and N.-S. Liou, "Hyperspectral imaging system with rotation platform for investigation of jujube skin defects," *Applied Sciences*, vol. 10, no. 8, p. 2851, 2020.

[17] D. A. Omondiagbe, S. Veeramani, and A. S. Sidhu, "Machine learning classification techniques for breast cancer diagnosis," in *IOP Conference Series: Materials Science and Engineering*, vol. 495, no. 1. IOP Publishing, 2019, p. 012033.

[18] A. Al-Zebari and A. Sengur, "Performance comparison of machine learning techniques on diabetes disease detection," in *2019 1st international informatics and software engineering conference (UBMYK)*. IEEE, 2019, pp. 1–4.

[19] N. Situ, X. Yuan, J. Chen, and G. Zouridakis, "Malignant melanoma detection by bag-of-features classification," in *2008 30th annual international conference of the IEEE engineering in medicine and biology society*. IEEE, 2008, pp. 3110–3113.

[20] D. Ruiz, V. Berenguer, A. Soriano, and B. Sánchez, "A decision support system for the diagnosis of melanoma: A comparative approach," *Expert Systems with Applications*, vol. 38, no. 12, pp. 15 217–15 223, 2011.

[21] M. A. Kassem, K. M. Hosny, R. Damaševičius, and M. M. Eltoukhy, "Machine learning and deep learning methods for skin lesion classification and diagnosis: A systematic review," *Diagnostics*, vol. 11, no. 8, p. 1390, 2021.

[22] Q. Abbas, "Content-based image retrieval system for clinical diagnosis of pigmented skin lesions," *IJCSNS*, vol. 17, no. 5, p. 238, 2017.

[23] P. Kharazmi, J. Zheng, H. Lui, Z. Jane Wang, and T. K. Lee, "A computer-aided decision support system for detection and localization of cutaneous vasculature in dermoscopy images via deep feature learning," *Journal of medical systems*, vol. 42, no. 2, pp. 1–11, 2018.

[24] J. Bandic, S. Kovacevic, R. Karabeg, A. Lazarov, and D. Opric, "Teledermoscopy for skin cancer prevention: a comparative study of clinical and teledermoscopic diagnosis," *Acta Informatica Medica*, vol. 28, no. 1, p. 37, 2020.

[25] S. Pathan, K. G. Prabhu, and P. Siddalingaswamy, "Techniques and algorithms for computer aided diagnosis of pigmented skin lesions—a review," *Biomedical Signal Processing and Control*, vol. 39, pp. 237–262, 2018.

[26] P. G. Cavalcanti and J. Scharcanski, "Automated prescreening of pigmented skin lesions using standard cameras," *Computerized Medical Imaging and Graphics*, vol. 35, no. 6, pp. 481–491, 2011.

[27] M. Ferri, I. Tomba, A. Visotti, and I. Stanganelli, "A feasibility study for a persistent homology-based k-nearest neighbor search algorithm in melanoma detection," *Journal of Mathematical Imaging and Vision*, vol. 57, no. 3, pp. 324–339, 2017.

[28] J. S. Lim, "Two-dimensional signal and image processing," *Englewood Cliffs*, 1990.

[29] N. Otsu, "A threshold selection method from gray-level histograms," *IEEE transactions on systems, man, and cybernetics*, vol. 9, no. 1, pp. 62–66, 1979.

[30] K. M. Nahar, B. Abul-Huda, A. Abu Naser, and R. M. Al-Khatib, "Twins and Similar Faces Recognition Using Geometric and Photometric Features with Transfer Learning," *International Journal of Computing and Digital System*, vol. 11, no. 01, 2022.

[31] C. Y. Wong, S. Liu, S. C. Liu, M. A. Rahman, S. C.-F. Lin, G. Jiang, N. Kwok, and H. Shi, "Image contrast enhancement using histogram equalization with maximum intensity coverage," *Journal of Modern Optics*, vol. 63, no. 16, pp. 1618–1629, 2016.

[32] I. G. Maglogiannis and E. P. Zafiropoulos, "Characterization of digital medical images utilizing support vector machines," *BMC Medical Informatics and Decision Making*, vol. 4, no. 1, pp. 1–9, 2004.

[33] A. Bono, S. Tomatis, C. Bartoli, G. Tragni, G. Radaelli, A. Maurichi, and R. Marchesini, "The abcd system of melanoma detection: A spectrophotometric analysis of the asymmetry, border, color, and dimension," *Cancer: Interdisciplinary International Journal of the American Cancer Society*, vol. 85, no. 1, pp. 72–77, 1999.

[34] V. T. Ng, B. Y. Fung, and T. K. Lee, "Determining the asymmetry of skin lesion with fuzzy borders," *Computers in biology and medicine*, vol. 35, no. 2, pp. 103–120, 2005.

[35] T. Satheeshsa, D. Sathyanarayana, and M. Giriprasad, "Detection of in-situ melanoma using symmetry of data and color spread factor," *International Journal of Engineering Research*, vol. 3, no. SP 2, pp. 64–67, 2014.

[36] H. Alquran, I. A. Qasmieh, A. M. Alqudah, S. Alhammouri, E. Alawneh, A. Abughazaleh, and F. Hasayen, "The melanoma skin cancer detection and classification using support vector machine," in *2017 IEEE Jordan Conference on Applied Electrical Engineering and Computing Technologies (AEECT)*. IEEE, 2017, pp. 1–5.

[37] H. Alquran, E. Shaheen, J. M. O'Connor, and M. Mahd, "Enhancement of 3d modeling and classification of microcalcifications in breast computed tomography (bct)," in *Medical Imaging 2014: Image Processing*, vol. 9034. SPIE, 2014, pp. 799–807.

[38] M. Cogswell, F. Ahmed, R. Girshick, L. Zitnick, and D. Batra, "Reducing overfitting in deep networks by decorrelating representations," *arXiv preprint arXiv:1511.06068*, 2015.

[39] N. Hameed, A. Shabut, and M. A. Hossain, "A computer-aided diagnosis system for classifying prominent skin lesions using machine learning," in *2018 10th Computer Science and Electronic Engineering (CEEC)*. IEEE, 2018, pp. 186–191.

Majd Tahat earnd his M.Sc. degree (2018) in Computer Information System at Yarmouk University Faculty of Information Technology and Computer Science. He holds a B.Sc. degree in Computer Information System from Yarmouk University (2013). Tahat has been a teacher assistant at Department of Computer Science in Jordan University of Science and Technology (2014). Where he currently work as a Senior Lecturer at The Arabic Council of Writers and Intellectuals since 2018 and he is giving courses in Artificial Intilegance and Machine Learning..

Belal Abuata obtained his BSc. in Computer Science from Yarmouk University, Jordan and MSc in Computer Science from the National University of Malaysia in. Also, he obtained his PhD degree from National University of Malaysia in the area of Multilingual Information Retrieval. He is presently working as Associate Professor in the Faculty of IT and Computer Sciences, at Yarmouk University, Jordan. He is having a total of more than 20 years of teaching experience and research in various IT colleges in Malaysia, Bahrain and Jordan. His research interest includes Information Retrieval, Web Searching and Evaluation, Multimedia Systems.

Maryam Nuser received the B.Sc. degree in computer science from Yarmouk University, Jordan, in 1995, and the M.Sc. and Ph.D. degrees from the University of Arkansas, USA, in 2002 and 2004, respectively. She was the Head of the CIS Department, Yarmouk University, from 2006 to 2008. She is currently an Associate Professor with the Information Systems Department, Faculty of Information Technology and Computer Sciences,Yarmouk University.